Cine MR-Based Radiomics to Predict Myocardial Segments With Infarction

Yongjia Peng
Jinan University
Yan Wang
University of California San Francisco
Kongyang Wu
Jinan University
Yan Luo
Jinan University
Jing Liu
University of California San Francisco
Yixiang Wang
Chinese University of Hong Kong
Jingshan Gong (jshgong@sina.com)
Jinan University

Research Article

Keywords: Myocardial Infarction, cine Magnetic Resonance, Radiomics

Posted Date: June 11th, 2021

DOI: https://doi.org/10.21203/rs.3.rs-583540/v1

Abstract

Background: Although myocardial infarction (MI) can be assessed quantitatively and qualitatively by using late gadolinium-enhanced (LGE) cardiovascular magnetic resonance (CMR) imaging, intravenous administration of gadolinium can expose patients to high risk of nephrogenic systemic fibrosis, especially in those with cardiovascular diseases. The purpose of this study is to harness cine CMR-based radiomics for predicting MI without introducing gadolinium.

Methods: In this retrospective study, we included 48 patients with acute myocardial infarction (AMI) confirmed by later gadolinium enhancement (LGE) at CMR. CMR examinations were performed within 2 to 6 days after PCI. According to the LGE, each myocardial segment was dichotomized into with and without MI. Radiomic features of myocardial segments were extracted from cine CMR images and the myocardial segments were divided into training and validation sets randomly at a ratio of 0.7:0.3. Pearson correlation and Mann-Whitney U rank test were used to eliminate redundant and irrelevant features. A least absolute shrinkage and selection operator (LASSO) algorithm was used for features selection in the training set. Radiomic signatures were constructed in both the training and validation sets and its predictive performance was assessed using area under the cure of receiver operating characteristic (AUC-ROC).

Results: Of 768 myocardial segments in the 48 patients, there were 291 (38%) segments with MI and 477 (62%) segments without MI. After univariate analysis, there were 22 RFs related to MI with statistical significance. LASSO regression selected 18 RFs for radiomics signature builting. AUC-ROC of radiomic signatures in prediction of segments with MI was 0.74(95% CI:0.69-0.78)and 0.68 (95%CI: 0.60-0.75) in the training and validation sets, respectively. The difference was not statistically significant (p=0.14).

Conclusion: Cine MR-based radiomics signature can achieve a good prediction performance for MI, which showed the potential to be a promising imaging biomarker for MI without the administration of contrast agent.

Indroduction

Emergency percutaneous coronary intervention (PCI) for myocardial salvage is the current standard of treatment in patients with acute ST segment elevation myocardial infarction (MI) [1]. Echocardiography can be used for immediate and readily bedside assessment of ventricular wall motion. Unfortunately, ventricular wall motion at rest cannot be used to quantify salvage early after infarction, as both necrotic and viable myocardium may demonstrate impaired regional myocardial contraction[2] and the severity of MI is a determining factor of left ventricular dysfunction and long-term remodeling [3]. Therefore, it is essential to identify the size of infarcted myocardium. Cardiovascular magnetic resonance (CMR) imaging, which can provide high spatial resolution contracture and functional images of heart, has obtained a widespread clinical acceptance in assessment of heart diseases. It is well known that late gadolinium enhanced (LGE, 10–15 min after contrast injection) CMR can demonstrate infarcted myocardium as an area of persistent enhancement[4–6]. The intravenous administration of gadolinium-based contrast agents is not only time-consuming, but also exposes the patients to potential high-risk of fatal adverse events, such as nephrogenic systemic fibrosis which occurs more common in patients with renal failure [7], because patients with coronary artery disease have a higher prevalence of coexisting chronic kidney disease than patients without coronary artery disease. In

order to overcome these drawbacks of contrast enhanced CMR, researchers tried to seek native quantitative parameters of non-contrast CMR for characterizing myocardium[8–10].. As myocardial edema occurs as early as 15 minutes after coronary occlusion, with a myocardial water content of 3–7% after occlusion that increases to 28% after myocardial reperfusion, T2 mapping can archive good diagnostic accuracy in identifying acute myocardial edema[11–12]. With the development of computer science and artificial intelligence, radiomics, which harness computer to high-thoroughly extract high-dimensional digital features of medical images, had become a promising discipline to bridge medical imaging and precision medicine. For the cine CMR sequence on the basis of T2 relaxation, we hypothesized that cine CMR images harbor features to identify MI. Perhaps these features are too trivial to be perceived by naked eyes. Therefore, the purpose of this study is to explore the feasibility of cine CMR-based radiomics to predict MI in patients after PCI to restore epicardial coronary blood flow.

Methods

Patients

This retrospective study was approved by the institutional review board of our hospital, and the requirement for informed consent was waived due to its retrospective nature. Eighty-five consecutive patients who underwent CMR within 2–6 days after PCI at Shenzhen People's Hospital from October 2017 to December 2020 were found in the hospital information system (HIS). Inclusion criteria were:(a) PCI was performed within 24 hours of onset of myocardial infarction symptoms or clinical diagnosis of AMI, and occluded vessels were successfully opened; (b) CMR was performed within 2–6 days after surgery; and (c) the CMR examination was completed successfully and the images could be read from Picture Archiving and Communication Systems (PACS). Exclusion criteria were: (a) history of PCI before this time; (b) inadequate quality for image segment; (c) failure of extracting radiomics features; (d) microvascular obstruction identified within the infarcted myocardium. Finally, 48 patients were included in this study (Fig. 1), including 43 males and 5 females with an age range of 28–75 years and an average age of 52.6 years.

Cine CMR and LGE imaging acquisition

CMR was performed on 3.0T MR system (Magnetom Skyra; Siemens Healthcare) and 18-channel cardiac phased-control coil, equipped with respiratory gating and ECG vector gating. Steady-state precession fast sequence was used to capture standard left ventricular (LV) short axis and LV two-chamber, three-chamber and four-chamber cine CMR. The parameters were TR 3.8ms, TE 1.4ms, FA 80.FOV 340 mm x 340 mm, matrix 139×208, layer thickness 8 mm, layer spacing 1.6 mm, breath hold scanning at the end of expiration, acquisition time 15 ~ 18s. Late gadolinium enhancement imaging was performed 10–15 min after the intravenous administration of a gadolinium-based contrast agent at a dose of 0.1mmol/kg, using a two-dimensional T1-weighted reverse recovery gradient echo sequence. Inversion times were individually selected from 250ms- 400ms to optimize the nulling of the unaffected myocardium. The other parameters were TR 7.6ms, TE 1.09ms, FA 20, FOV 340 mm× 340 mm, matrix 128×128, layer thickness 8 mm, layer spacing 1.6 mm.

Image analysis and radiomics features extraction

Two experienced diagnostic radiologists (with more than 5-year-experience in reading CMR images) interpreted CMR images on the PACS (picture archiving and communication system) in consensus. MI was defined as an area of persistent enhancement at LGE images. Myocardium segments were conducted using the American Heart Association proposed 16-segment model. 768 myocardial segments were obtained and each segment was dichotomized into with and without MI. The cine CMR images were downloaded from PACS and transferred into the ITK-SNAP (http://www.itksnap.org) software. The end-diastolic phase images were used for myocardium segmentation. The region of interest (ROI) was manually delineated around the boundary of the 16 segments of the left myocardium by the other two radiologists with more 5-year-experience in reading CMR images. Radiomic features were extracted by using the open-source software Pyradiomics package. The flow diagram of the patient selection and radiomics features extraction process is displayed in Fig. 2. In the end, 105 texture features were obtained, with the feature names and numbers as follows:14 shape-based features, 16 First Order Statistics features, 24 Gray Level Co-occurrence Matrix (GLCM) features, 16 Gray Level Run Length Matrix (GLRLM) features, 16 Gray Level Size Zone (GLSZM) features, 16 Gray Level Size Zone (GLSZM) features, 5 Neigbouring Gray Tone Difference Matrix (NGTDM) features and 14 Gray Level Dependence Matrix (GLDM) features.

Statistical analysis

Statistical analysis was performed using R software version 4.0.0 (http://www.r-project.org) and SPSS. A p value of less than 0.05 indicated statistical significance. The procession of feature selection and dimension reduction were following: first, intra-class correlation coefficients (ICCs) was used to excluded features with low reproducibility (ICC < 0.75) and average of the included features of two radiologists' segmentation was calculated; second, Pearson correlation coefficient was used to exclude those features highly correlated to each other (if two features were high correlated [r > 0.8], the one with lower area under the curve [AUC] of receiver operating characteristic [ROC]) was removed); third, Mann-Whitney U rank test was used to select those features which were associated with MI with statistical significance. Then, the 768 myocardial segments in the 48 patients were divided into training and test sets at a ratio of 0.7:0.3 randomly. The selected features were normalized separately using min-max normalization to reduce the impact of different scales. A least absolute shrinkage and selection operator (LASSO) regression with 10-fold cross-validation was employed to select the strongest features in the training set. Subsequently, these finally selected features were used to build radiomics signature. Predictive performance of radiomics signature for MI was evaluated in both the training and test sets using AUC of ROC. The AUCs were compared with the DeLong test using the 'pROC' package in R.

Results

Of the total 768 myocardial segments in the 48 patient, there were 291 (38%) segments with MI and 477 (62%) segments. ICCs and Pearson correlation coefficient excluded 83 features. Univariate analysis revealed that 22 features were statistically associated with MI. 18 of the 22 features were selected by the LASSO regression and used for radiomics signature development. These 18 features included 4 shape features, 2 first order

features, 3 GLCM feature, 2 GLSZM features, 5 GLDM feaures ,one GLRLM feature and one NGTDM feature (Table 1). According to the 18 radiomics features, radiomics signature was calculated according to:

radiomics signature=-3.47+-0.08*Maximum2DDiameterColumn + 0.30* Maximum2DDiameterRow+-1.43*Sphericity + 0.27*SurfaceVolumeRatio + 5.41*10Percentile+-4.60*90Percentile + 0.71*Correlation+-1.91*DifferenceEntropy+-1.14*Idmn + 3.04*RunEntropy + 1.17*LargeAreaHighGrayLevelEmphasis + 1.33*ZoneEntropy + 7.10*DependenceNonUniformity+-1.29*DependenceNonUniformityNormalized+-4.55*GrayLevelNonUniformity + 3.70*LargeDependenceEmphasis + 0.82*SmallDependenceLowGrayLevelEmphasis + 0.58*Coarseness

Radiomics signature of segments with MI was higher than that of segments without MI in the training set (−0.19 ± 0.91 vs -0.94 ± 0.80, $p < 0.001$). The highest three features with positive λ coefficient were GLDM_DependenceNonUniformity (λ = 7.10), followed by first order_10Percentile(λ = 5.41) and GLRLM_RunEntropy (λ = 3.03). The two features with negative λ coefficient and largest scale were GLDM _GrayLevelNonUniformity (λ=-4.55) and First order_90Percentile (λ=-4.60). AUCs of 0.74(95% CI: 0.69–0.78) and 0.68 (95%CI: 0.60–0.75) were obtained in the training and validation sets, respectively ($p = 0.14$, Fig. 3).

Table 1
The 18 radiomics features for radiomics signature development and their clinical meaning

Radiomic Features	λ coefficient	Clinical meaning
Shape feature_Maximum2DDiameterColumn	-0.08	A measure of the largest pairwise Euclidean distance between tumor surface mesh vertices in coronal plane
Shape feature _Maximum2DDiameterRow	0.30	A measure of the largest pairwise Euclidean distance between tumor surface mesh vertices in sagittal plane
Shape feature_Sphericity	-1.43	A measure of the roundness of the ROI relative to a circle
Shape feature_SurfaceVolumeRatio	0.27	a lower value indicates a more compact (circle-like) shape
First order_10Percentile	5.41	Strength values that account for 10% of ROI
First order_90Percentile	-4.60	Strength values that account for 90% of ROI
GLCM_Correlation	0.71	The linear dependency of gray level values to their respective voxels in the GLCM.
GLCM _DifferenceEntropy	-1.91	A measure of heterogeneity that places higher weights on differing intensity level pairs that deviate more from the mean
GLCM _Idmn	-1.14	A measure of the local homogeneity of an image.
GLRLM_RunEntropy	3.04	A measure of the uncertainty/randomness in the distribution of run lengths and gray levels. A higher value indicates more heterogeneity in the texture patterns.
GLSZM_LargeAreaHighGrayLevelEmphasis	1.17	a measure of the local homogeneity of an image
GLSZM _ZoneEntropy	1.33	A measure of the uncertainty/randomness in the distribution of zone sizes and gray levels
GLDM_DependenceNonUniformity	7.10	A measure of the similarity of dependence throughout the image, with a lower value indicating more homogeneity among dependencies in the image
GLDM _DependenceNonUniformityNormalized	-1.29	A measure of the similarity of dependence throughout the image, with a lower value indicating more homogeneity among dependencies in the image
GLDM _GrayLevelNonUniformity	-4.55	A measure of the similarity of gray-level intensity values in the image, where a lower GLN value correlates with a greater similarity in intensity values.

Radiomic Features	λ coefficient	Clinical meaning
GLDM _LargeDependenceEmphasis	3.70	A measure of the similarity of gray-level intensity values in the image, where a lower GLN value correlates with a greater similarity in intensity values.
GLDM _SmallDependenceLowGrayLevelEmphasis	0.82	A measure of the joint distribution of small dependence with lower gray-level values
NGLDM _Coarseness	0.58	A measure of average difference between the center voxel and its neighbourhood and is an indication of the spatial rate of change. A higher value indicates a lower spatial change rate and a locally more uniform texture.

Disscusion

In this study, we derived of radiomics signature from cine CMR images to predict MI. Our study showed that the cine CMR-based radiomics signature yielded moderately high predictive performance with AUCs of 0.74 and 0.68 in training and validation sets, respectively. In the training set, radiomics signature of myocardial segments with MI was higher than that of those without MI with statistical significance (− 0.19 ± 0.91 vs -0.94 ± 0.80, $p < 0.001$).

Administration of contrast materials can be fatal to patients with acute myocardial infarction, for they often coexist chronic kidney disease. As myocardial infarction accompanies water content, T2 relaxation might be prolonged. Cine CMR imaging is one of the most common CMR sequences for heart function assessment. It bases on steady state free precession, which is a gradient recall echo sequence addressing T2 relaxatio. Therefore, it can reflect T2 relaxation change. Recently, Bustin and colleagues developed a single-shot T2-prepared balanced SSFP sequence to obtain 3D T2 mapping of myocardium[13]. They observed that focal areas of increased T2 values in patients with myocarditis, which well agreed with LGE findings. To best of our knowledge, this is the first study to harness routine cine CMR-based radiomics signature to predict MI in patients with AMI. Although the predictive performance was still moderate. Our study confirmed that radiomics can mine high dimension features beyond human eye perceive ability from the conventional non-contrast-enhanced images at some special fields in the real world to overcome some clinical dilemma. Among the 18 selected features, GLDM_DependenceNonUniformity, first order_10Percentile and GLRLM_RunEntropy were the top three features with positive λ coefficient, while GLDM _GrayLevelNonUniformity and First order_90Percentile had the largest two scales with negative λ coefficient. Therefore, a segment with more heterogeneous texture and high signal intensity indicates the possibility of harboring MI, while homogeneous texture and low signal intensity favor a segment without MI. This phenomenon could be interpreted as prolonging T2 relaxation due to edema after MI. If a segment harbored infarcted and normal myocardium, its texture would be more heterogeneous.

There were several limitations of this study. First, this was a retrospective study, which included those patients with LGE proven MI. Therefore, selection bias was introduced inevitably. Second, due of a small group of patients with MI, we performed analysis about per segment instead of regarding patient, so that clinical

variables and offensive vascular were not taken into account. Integrating easy available clinical data might improve predictive performance. Third, this primary study was performed at single center with small sample size, further test cohort from broad available institutes will be required to validate the possibility and usefulness of cine CMR-based radiomics signature to be a surrogate biomarker for MI.

In conclusion, the cine CMR-based radiomics signature showed moderately high predictive performance for MI. This primary single center study throw light on the possibility of harnessing routine cine CMR images to build radiomics signature as a surrogate biomarker for MI.

Abbreviations

AMI= acute myocardial infarction

MI= myocardial infarction

PCI =percutaneous coronary intervention

CMR =Cardiovascular magnetic resonance

LGE= late gadolinium enhanced

ROI= region of interest

GLCM =Gray Level Co-occurrence Matrix

GLRLM= Gray Level Run Length Matrix

GLSZM=Gray Level Size Zone

GLSZM=Gray Level Size Zone

NGTDM=Neigbouring Gray Tone Difference Matrix

(GLDM= Gray Level Dependence Matrix

ICCs =intra-class correlation coefficients

AUC =area under the curve

ROC= receiver operating characteristic

LASSO= least absolute shrinkage and selection operator

PACS=picture archiving and communication system

HIS= hospital information system

Declarations

Ethics approval and consent to participate: This retrospective study was approved by the institutional review board of our hospital. and the requirement for informed consent was waived due to its retrospective nature.

Consent for publication: During MRI examinations, the patients had signed an informed consent, which included to agree that their MR images can be used for research and publish.

Availability of data and materials: The datasets used and/or analysed during the current study are available from the corresponding author on reasonable request.

Competing interests: The authors declare that they have no competing interests

Funding: The Shenzhen Science and Technology Project supported this study (No. GJHZ20180928172002087).

Authors' contributions: J.P and Y.L segmented images and extracted the radiomics features. K.W carried out statistical analysis and radiomics signature building. Y.W and J.G wrote the manuscript text. J.L and Y.W revised the manuscript text. All the authors reviewed the manuscript.

Acknowledgements: Not applicable

References

1. Gershlick AH, Banning AP, Myat A, Verheugt FW, Gersh BJ. Reperfusion therapy for STEMI: is there still a role for thrombolysis in the era of primary percutaneous coronary intervention? Lancet 2013;382(9892):624–632.
2. Mazeika PK, Nadazdin A, Oakley CM. Dobutamine stress echocardiography for detection and assessment of coronary artery disease. J Am Coll Cardiol 1992;19:1203–1211
3. Symons R, Masci PG, Goetschalckx K, Doulaptsis K, Janssens S, Bogaert J. Effect of infarct severity on regional and global left ventricular remodeling in patients with successfully reperfused ST segment elevation myocardial infarction. Radiology. 2015 Jan;274(1):93–102.
4. Simonetti OP, Kim RJ, Fieno DS, et al. An improved MR imaging technique for the visualization of myocardial infarction. Radiology 2001;218:215–223.
5. Ichikawa Y, Sakuma H, Suzawa N, Kitagawa K, Makino K, Hirano T, Takeda K. Late gadolinium-enhanced magnetic resonance imaging in acute and chronic myocardial infarction. Improved prediction of regional myocardial contraction in the chronic state by measuring thickness of nonenhanced myocardium. J Am Coll Cardiol. 2005 Mar 15;45(6):901–9.
6. Klein C, Schmal TR, Nekolla SG, Schnackenburg B, Fleck E, Nagel E. Mechanism of late gadolinium enhancement in patients with acute myocardial infarction. J Cardiovasc Magn Reson. 2007;9(4):653–8.
7. Bruce R, Wentland AL, Haemel AK, et al. Incidence of Nephrogenic Systemic Fibrosis Using Gadobenate Dimeglumine in 1423 Patients With Renal Insufficiency Compared With Gadodiamide. Invest Radiol 2016;51(11):701–705
8. Tahir E, Sinn M, Bohnen S, et al. Acute versus Chronic Myocardial Infarction: Diagnostic Accuracy of Quantitative Native T1 and T2 Mapping versus Assessment of Edema on Standard T2-weighted

Cardiovascular MR Images for Differentiation[J]. Radiology.2017 Oct;285(1):83–91.

9. Gottbrecht M, Kramer CM, Salerno M. Native T1 and Extracellular Volume Measurements by Cardiac MRI in Healthy Adults: A Meta-Analysis[J]. Radiology. 2019 Feb;290(2):317–326.
10. Tahir E, Sinn M, Bohnen S, et al. Acute versus Chronic Myocardial Infarction: Diagnostic Accuracy of Quantitative Native T1 and T2 Mapping versus Assessment of Edema on Standard T2-weighted Cardiovascular MR Images for Differentiation[J]. Radiology. 2017 Oct;285(1):83–91.
11. García-Dorado D, Oliveras J, Gili J, et al. Analysis of myocardial oedema by magnetic resonance imaging early after coronary artery occlusion with or without reperfusion[J]. Cardiovasc Res. 1993 Aug;27(8):1462–9.
12. Park CH, Choi EY, Kwon HM, et al. Quantitative T2 mapping for detecting myocardial edema after reperfusion of myocardial infarction: validation and comparison with T2-weighted images[J]. Int J Cardiovasc Imaging. 2013 Jun;29 Suppl 1:65–72.
13. Bustin A, Hua A, Milotta G, et al. High-Spatial-Resolution 3D Whole-Heart MRI T2 Mapping for Assessment of Myocarditis[J]. Radiology. 2021 Mar;298(3):578–586.

Figures

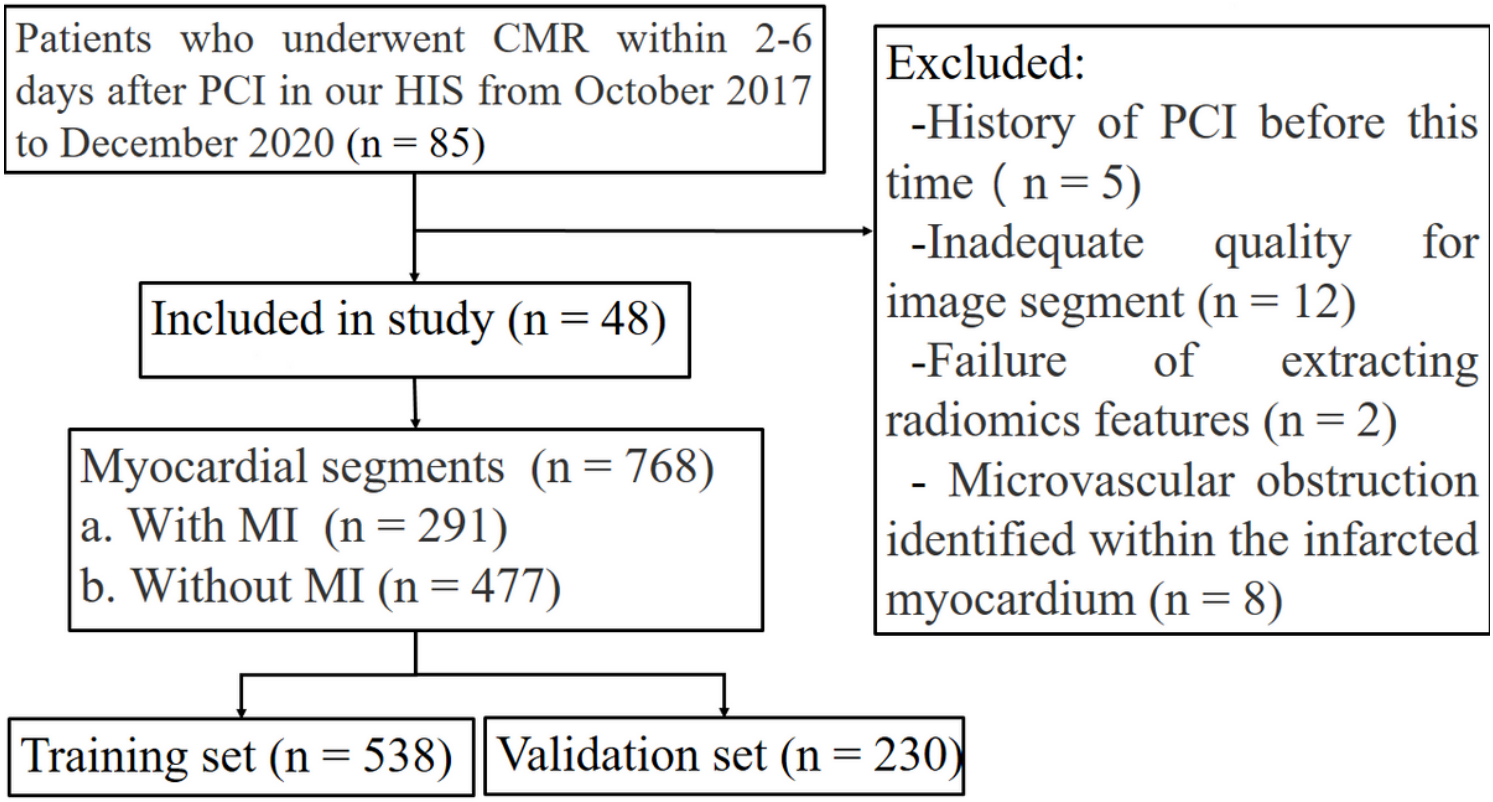

Figure 1

Flowchart of the patient selection process.

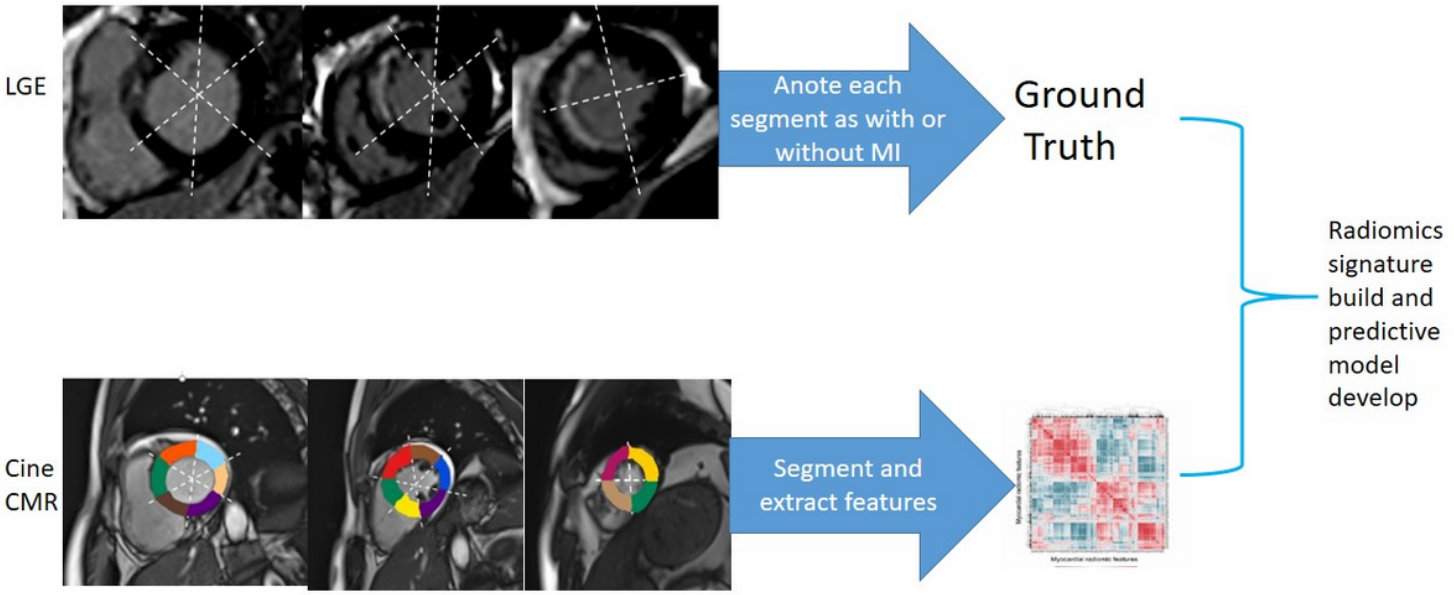

Figure 2

The workflow of the radiomics analysis of myocardial segments.

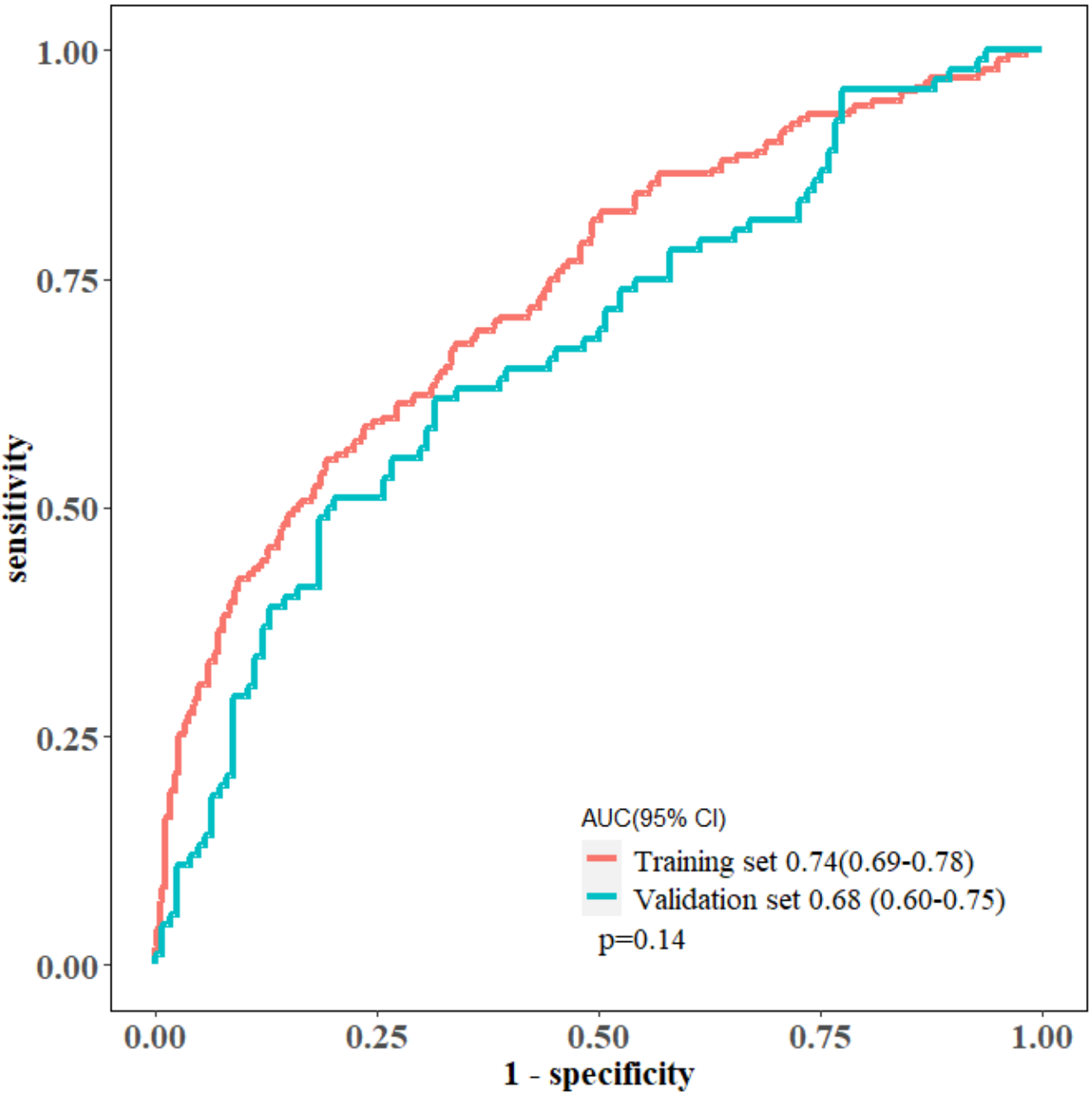

Figure 3

Radiomics signature of segments with MI and without MI in the training set